Creation of Digital Bathymetric Maps using High Resolution Satellite Imagery and Multispectral Bathymetric Modeling for Shallow Waters

M. Papadopoulou[1], P. Lafazani[1], E.R. Mavridou[2], M. Tsakiri-Strati[3], G. Doxani[2]

1 Laboratory of Cadastre and GIS, School of Rural and Surveying Engineering, AUTH
2 Rural and Surveying Engineer, AUTH
3 Laboratory of Photogrammetry and Remote Sensing, School of Rural and Surveying Engineering, AUTH

Abstract: In this paper the procedure of creating bathymetric maps using techniques of multispectral bathymetry was investigated. High resolution IKONOS -2 imagery data and the Lyzenga linear bathymetry model were used. For the calibration of the depth model the multispectral image information was integrated with available echo sounding data. Prior to the model's calibration the glint correction according to Hedley's method and a crude atmospheric correction based on the "dark pixel subtraction" over the sea area took place. The existence of sea grass in a part of the study area influenced the relationship between water reflectance and depth. Therefore, the study area was divided into three different parts and the bathymetric model was applied in: (a) an area with sea grass, (b) a sandy area and (c) a mixed area. The corresponding calibrated models were used to give a depth value to each pixel in every subarea. This way, a depth surface for every part was formed and the corresponding depth contours were drawn. For the removal of noise in the produced depths, and the final form of the contours, low pass spatial filtering techniques for raster data and line smoothing techniques for vector data were applied. The purpose of this study was on the one hand the exploitation of the multispectral bathymetry techniques in order digital depth contour maps to be created and on the other hand the locating of problems and factors that import uncertainty in the various steps of the procedure.

1. Introduction

Accurate bathymetric measurements are considered of fundamental importance towards monitoring sea bottom and producing nautical charts in support of marine navigation (Stumpf et al., 2003, Su et al., 2008). Until recently, bathymetric surveying of shallow sea water has been mainly based on conventional ship-borne echo sounding operations. However, this technique demands cost and time, particularly in shallow waters, where a dense network of measured points is required. The last decades remotely sensed data have provided a cost- and time-effective solution

to sufficiently accurate depth estimation (Lyzenga, 1985, Stumpf et al., 2003, Su et al., 2008). The initial attempts for automatic estimation of water depth were based on the combination of aerial multispectral data and radiometric techniques (Lyzenga, 1978). With the advent of Landsat images, the methods of monitoring sea floor were increased, so as to be efficiently applied on optical satellite images (Lyzenga, 1981, Spitzer and Dirks, 1987, Philpot, 1989, Van Hengel and Spitzer, 1991). In the following years, the advance of remote sensing technology expanded the use of these methodologies to data with improved spatial and spectral resolution, i.e. Ikonos (Stumpf et al., 2003, Mishra et al. 2007, Su et al., 2008), Quickbird (Lyons et al., 2011) and Worldview-2 data (Kerr, 2010, Bramante et al., 2010, Doxani et al., 2012). A wide variety of empirical models has been proposed and evaluated for bathymetric estimations by establishing the statistical relationship between image pixel values and field measured water depth values. The most popular approach was proposed by Lyzenga (1978, 1981, 1985) and was based on the fact that the bottom-reflected reflectance is approximately a linear function of the bottom reflectance and an exponential function of the water depth. The main hindrances while applying these processes are reflectance penetration and water turbidity (Su et al., 2008). The implementation and the accuracy of this process is also impeded by the appearance of glint as well as clouds, the prevailing atmospheric conditions and the existence of various kinds of spectral noise. The result of the multispectral bathymetry is a raster surface of depths that needs a further elaboration towards the creation of bathymetry contours. As shown in the following paragraphs low pass filtering techniques have to be applied to clear the "cartographic" noise that is due to image resolution and/or the factors mentioned above. The purpose of this study is on the one hand the description of a procedure that starts from multispectral bathymetry techniques and ends with the forming of reliable digital depth contours and on the other hand the locating of problems and factors that import uncertainty in the various steps of this procedure. For the implementation of this study the IBM SPSS Statistics 19.0, the IMAGINE ERDAS 9.2 and ArcGIS 9.3.1 software packages were used.

2. Imagery data and study area

The depth estimation concerns the coastal area of Nea Michaniona, Thessaloniki, in the northern part of Greece. The sea bottom changes very smoothly and the water is clear (Hatzigaki et al., 2000). The shallower parts are covered with dense sea grass while the deeper area is sandy (Figure 1).

The four bands of Ikonos-2 multispectral image (blue, green, red, near infrared) with spatial resolution of 1m and acquisition date the 1st of September 2007 involved in this study. From now on the four bands of the image will be called band 1(blue), band 2 (green), band 3 (red) and band 4 (NIR).The available data were

Figure 1. *(a) location of the study area in the whole of Greece and the Nea Michaniona area, (b) location of the study area (red frame) in the whole of Ikonos-2 image (R:4, G:3, B:2) (c) the actual study area (blue frame) where the land has been cut off (R:4, G:3, B:2).*

geo-referenced to UTM (zone 34) system and WGS84 (see e.g. Fotiou and Pikridas, 2006). As it can be easily seen in Figure 1b, there is evident cloudiness in the wider area of interest but not in the actual study area (Figure 1c) where however there is significant radiometric stripe noise as well as sun glint. The noise was not corrected since its correction could become a considerable factor of uncertainty in the calibration of the bathymetry model and a thorough study would be needed in order the correction method would not create adverse changes in the reflectance. Therefore the stripe noise remained and its effect on the model's calibration was just observed. It is of course understandable, that in order an image to be used for bathymetric applications it must be chosen with high caution so that the sea area is absolutely free of such noise. According to the above, the preparation of the image related only to the glint removal and to atmospheric correction, which is also necessary in preparing of the image. For a more accurate atmospheric correction and removal of the glint, only the sea was kept and the land was cut off (Figure 3c).

The linear bathymetry model was calibrated using echo sounding data in UTM (zone 34) and WGS84. The survey of the bottom was accomplished through measurements of depths from 3.5 m to 15.0 m and GPS corresponding horizontal positions on a calm sea surface. The internal accuracy of depth measurements reached the 10 cm. (Hatzigaki et al., 2000).

3. Sun glint correction

Hedley et al. (2005) introduced a simplified and robust methodology for the sun glint correction. The suggestion was the use of one or more samples of the image. The image processing for glint correction involves a linear regression analysis between the sample pixels of every visible band (y-axis) and the corresponding pixels of band 4 (x-axis). This method is usually applied after atmospheric correction, but if the atmospheric conditions are considered uniform all over the study area it can be used at first.

The image pixels are corrected according to the following equation:

$$R_i^{'} = R_i - b_i(R_{NIR} - Min_{NIR}) \quad (1)$$

where $R_i^{'}$ = the corrected pixel value, R_i = the initial pixel value, b_i = the regression line slope , R_{NIR} = the corresponding pixel value in band 4 and Min_{NIR} = the minimum value of band 4 existing in the sample.

The methodology was implemented for 7500 sample pixels (Doxani et al., 2013). The sample positions are depicted in Figure 2a.

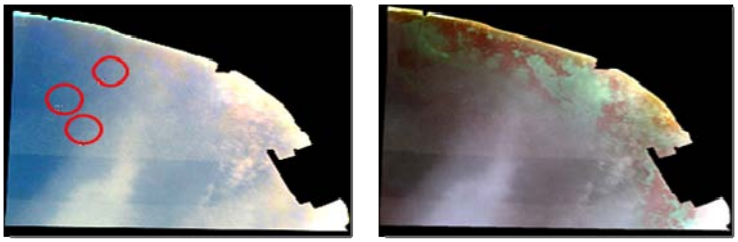

Figure 2. *The study area (R:4, G:3, B:2) (a) before the removal of glint. The places of the image samples are depicted (red circles), (b) after the removal of glint*

4. Atmospheric correction and calibration of the Lyzenga model

4.1. Atmospheric correction

There is a wide variety of methods for atmospheric correction above the sea surface. However, they usually require some input parameters concerning atmospheric and sea water conditions that are difficult to be obtained (Kerr, 2010). For this reason the simplified method of dark pixel subtraction is usually preferred for this kind of application (Benny and Dawson, 1983, Green et al., 2000, Mishra et al., 2007). The atmospherically corrected pixel value Rac is then:

$$Rac = Ri - Rdp \quad (2)$$

where Ri = the initial pixel value Rdp = the dark pixel value

According to Benny and Dawson (1983) the dark pixel value subtraction is valid if the atmospheric behaviour is constant for the whole study area. The disadvantage of this crude method is the fact that the dark pixel value can be determined in various ways (e.g. Lyzenga, 1981, Benny and Dawson, 1983, Green et al., 2000, Edwards, 2010) that result in different correction values. An unsuccessful determination of Rdp may affect the depth estimation (Stumpf et al., 2003). An additional drawback appears in cases where the bottom reflectance is lower than the dark

pixel value, for instance when the bottom is covered with sea grass, and the difference in equation (2) becomes negative. Consequently equation (3) in §4.2 cannot be satisfied.

The atmospheric correction through the subtraction of the dark pixel value followed the glint correction. In order to avoid negative differences between the image pixels and the dark pixel value, the histogramme of every band was examined and a cut-off at its lower end was spotted. The value corresponding to this cut-off was considered as the dark pixel value (Benny and Dawson, 1983, Hatzigaki et al., 2000, Doxani et al, 2012). An Rdp value was defined for every band.

4.2. The Lyzenga bathymetry model

Lyzenga (1978) described the relationship between an observed reflectance Rw and the corresponding water depth z and bottom reflectance Ad as:

$$Rw = (Ad - Rw)\exp(-gz) + Rdp \quad (3)$$

where Rdp = dark pixel value, g = a function of the attenuation coefficients.

Rearranging equation (3) depth z can be described as (Stumpf et al., 2003):

$$z = g^{-1}[\ln(Ad - Rw) - \ln(Rw - Rdp)] \quad (4)$$

where $(Rw - Rdp) >= 0$

This single band method for depth estimation assumes that the bottom is homogeneous and the water quality is uniform for the whole study area. Lyzenga (1978, 1985) showed that using two bands could correct the errors coming from different bottom types provided that the ratio of the bottom reflectance between the two bands for all bottom types is constant over the scene. The proposed model is (Lyzenga, 1985):

$$z = a_0 + a_i \ln(Rac_i) + a_j \ln(Rac_j) \quad (5)$$

where a_0, a_i, a_j are coefficients determined through multiple regression and Rac_i and Rac_j are the corrected from atmospheric effects reflectance values.

Lyzenga et al. (2006) proved that the N-band model

$$z = a_0 + \sum_{i=1}^{N} a_i \ln(Rac_i) \quad (6)$$

although derived under the assumption that the water optical properties are uniform (Lyzenga 1978, 1985) gives depths that are not influenced by variations in water properties and/or bottom reflectance. This means that the more the available bands are, the better the depth estimation. According to Bramante et al. (2010) imagery data with multiplicity of bands, should produce better results over heterogeneous study areas. During the last three decades several bathymetry applications were

accomplished based on the above model. Two or more bands of low or high resolution passive images were tested in an effort to remove errors due to bottom and/or water quality differences producing quite satisfying results (Lyzenga, 1985; van Hengel and Spietzer, 1988, Papadopoulou and Tsakiri-Strati, 1998, Hatzigaki et al., 2000, Stumpf et al., 2003, Lyzenga, 2006, Bramante et al., 2010, Lyons et al., 2011).

4.3. Calibration of the bathymetric model

Taking as dependent variable the depth of each known point in the whole of the study area and as independent variables the corresponding natural logarithm of the corrected radiation for each band, a stepwise regression (e.g. Lafazani, 2003) was performed twice, in order the statistical indices of the regression to be ameliorated. Indicatively, the best R^2 was equal to 0.542, a non-acceptable value and the Durbin-Watson index was a little more improved with the second regression reaching the value 0.909. Further regressions gave similar statistical results (Mavridou, 2013). Moreover, the scatter plots (Figure 3) between the depth and each of the natural logarithms of the corrected bands show that there is no obvious linear relationship between the dependent and independent variables. Despite what was said in §4.2, about the multiplicity of bands that contributes to overcoming the problem of heterogeneous bottom types, the calibration of linear model in the whole of the study area was not statistically proper. Thus, it was decided, just as in Doxani et al.,

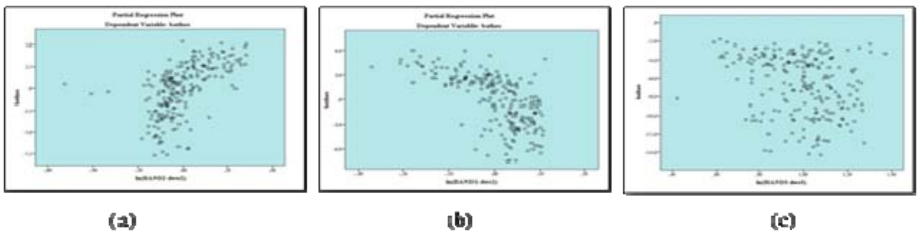

Figure 3. *Scatter plots between (a) depth and ln(Rac_2) b) depth and and ln(Rac_1) (c) depth and ln(Rac_3)*

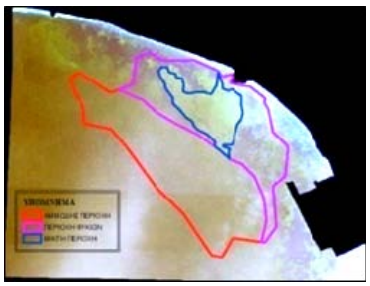

Figure 4. *The three study subareas. The red frame encloses the sandy area with deep water, the blue frame encloses the mixed area and the magenta frame encloses the area that is covered with sea grass*

2012, the study area to be divided into three different sub-regions with uniform or almost uniform bottom and the linear model to be calibrated separately for each region The three areas are the sea grass area with the shallower waters, the sandy area with the deeper waters and the mixed area with intermediate depths (Figure 4).

4.3.1 Calibration of bathymetric model in the sea grass area

The process of regression to calibrate the model was repeated five times. After sequential statistical tests and the removal of leverages the final model (7) is given by the following equations with $R_2 = 0.728$ and Durbin-Watson 1.535 (Mavridou, 2013)

$$\hat{Y} = -13{,}327 \times \ln(Rac_1) + 5.203 \times \ln(Rac_2) + 16.085 \quad (7)$$

where $\hat{Y}$ is the predicted depth and Rac_1, Rac_2 are the corrected from atmospheric effects reflectance values in band 1 and band 2.

In this model only bands 1 and 2 participated. The evaluation of the model was performed with control points of known depth, whose predicted values were calculated according to (7). In the beginning, using the points of the calibration of the model the graph of Figure 5 was created as follows (Doxani et al., 2012, Mavridou, 2013):

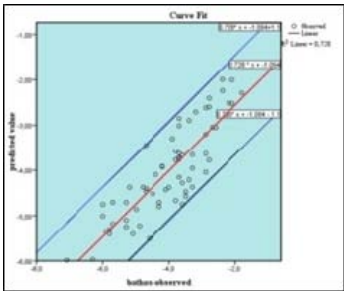

Figure 5. *The graphic expression of confidence zone. The blue lines represent the limits of the confidence interval.*

The line that has the best fit to the data was calculated. This line is expressed by the equation:

$$\hat{Y} = -1.094 + 0.728Y \quad (8)$$

where $\hat{Y}$ is the predicted depth and Y is the measured depth. After that, the (9) and (10) that define the limits of the zone of 95% confidence, were graphically calculated parallel to the line (8).

$$\text{upper limit: } Y_1 = -1.094 + 0.728Y + 1.10 \quad (9)$$

$$\text{lower limit: } Y_2 = -1.094 + 0.728Y - 1.10 \quad (10)$$

For every control point the variables Y_1 και Y_2 were calculated according to (9) and (10) where $Y = \hat{Y}_{pred}$ that is the predicted depth value of the control point.

Actually, variables Y_1 and Y_2 represent the limits of the confidence interval for the depth value calculated by the regression.

The evaluation of the model was made by comparing the measured depth values of control points to variables Y_1 and Y_2. Acceptable are the control points that satisfy the following inequality:

$$Y_2 < \text{measured depth} < Y_1 \quad (11)$$

Only 26,40% of the control points were found outside the confidence interval. For the other points within the confidence interval, a 42% introduced difference between the measured and the estimated depth less than 0.5m. The calibration of the model was considered satisfactory.

4.3.2 Calibration of bathymetric model in the sandy area

The same methodology was followed for the calibration of the model in this area. Nine stepwise regressions took place and after sequential statistical tests and the removal of leverages the calibrated model resulted as described by (12) with R^2 0.565 and Durbin-Watson 1,207 (Mavridou, 2013). The values of these indices are not considered satisfactory but the continuation of the procedure and the removal of more leverages did not improve them.

$$\hat{Y} = 24{,}583 \times \ln(Rac_2) - 2{,}231 \times \ln(Rac_3) - 53{,}494 \quad (12)$$

where $\hat{Y}$ is the predicted depth and Rac_2, Rac_3 are the corrected reflectance values in band 2 and band 3.

In this model only bands 2 and 3 participated. The evaluation of the model was performed with control points of known depth, whose predicted values were calculated according to (12). The methodology described in the previous paragraph was followed. A 22.5% of the control points where outside the 95% confidence interval of the model. However, only a 21% of the points inside the confidence interval introduced a difference between measured and predicted depth less than 0.5m. The calibration was not considered satisfactory.

4.3.3 Calibration of bathymetric model in the mixed area

Four stepwise regressions took place and after sequential statistical tests and the removal of leverages the calibrated model resulted as described by (13) with R^2

0.743 and Durbin-Watson 1,733 (Mavridou, 2013). In this area only band 2 participated.

$$\hat{Y} = 5{,}528 \times \ln(\mathrm{Rac}_2) - 15{,}542 \tag{13}$$

where $\hat{Y}$ is the predicted depth and Rac_2 is the corrected reflectance in band 2

Because the final model (13) consists of the dependent variable and only one independent, the evaluation was made directly from (13). The absolute differences between predicted and measured depths ranged from 0.03 to 2,66 m. A percentage of 66.3% presented a difference less than 0.5 m. According to the depth differences, the evaluation of the model can be considered acceptable.

5. Creation of digital bathymetric maps

5.1. Raster and contour bathymetric maps

The final calibrated model for every region was used for the calculation of the depth for each pixel of every subarea. Thus, the corresponding raster map was produced (Figure 6a). The contours were designed with 1m interval because the seabed alters smoothly (§2) and the specific interval illustrates with consistency the degree of inclination of the bottom. Indicatively, in Figure 6 the depth surface and the corresponding contour map of the mixed area are depicted. The same valid for the other two subareas.

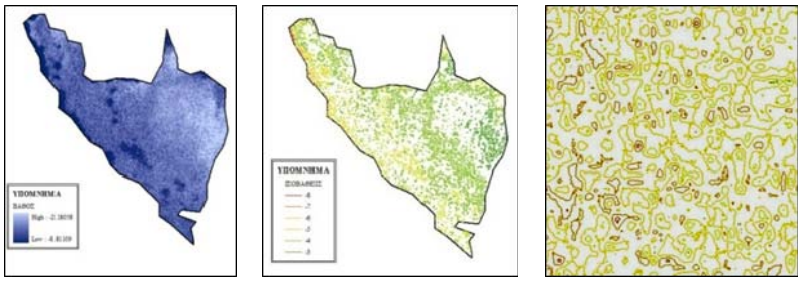

(a) *(b)* *(c)*

Figure 6. *The mixed area: (a) The depth surface which was produced using the calibrated linear model. (b) depth contours with 1m interval produced from the depth surface (c) detail from the depth contours. The "noise" in the data is evident.*

From Figure 6c it is obvious that the contour map contains noise. This is due to the small size of the pixels and since each one of them has different reflectance values, the model gives different depths. Furthermore, always an important factor for the production of depths is the reliability of the final calibrated model which most of the times does not give the same or about the same depth values in neighboring

pixels as it should in such a smoothly changing bottom. To obtain a map with useable information, the smoothing of the depth raster surface using low-pass filters (see e.g. Conzales, 1987, McCoy et al., 2002) is required and after that the smoothing of the bathymetric lines (see e.g. Li, 2007) that result from the filtered surface. However, both methodologies require special attention during their implementation since very easily a wrong choice of a smoothing filter or a line smoothing algorithm can eliminate not only the noise but also useful information.

5.2 Smoothing of the depth surface and the contour lines

The smoothing of the depth surface was performed using spatial low pass filters of the mean value. Various filters with different size and shape of neighborhood were tested, always targeting the elimination of noise. Finally the circle spatial filter was used (see e.g. McCoy et al. 2002), with a radius that varied from one subarea to another (Figure 7a). Using the smoothed surfaces fewer and clearer contours were created (Figures7b).

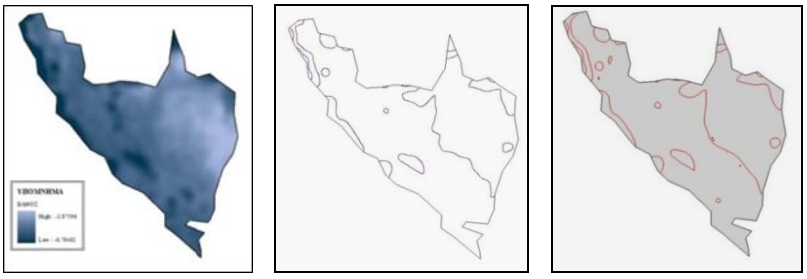

(a) *(b)* *(c)*

Figure 7. *The mixed area: (a) smoothed raster surface after using a circle spatial filter with a radius of 10 pixels, (b) contours as they come from the smoothed raster (c) smoothed contours after PAE K with a tolerance of 200m.*

These contours described the variation of depth sufficiently. However, due to their origin from the dense raster surface the contours had a "noisy" form and they had in their turn to be smoothed. For their smoothing the Polynomial Approximation with Exponential Kernel (PAEK) (ESRI) algorithm was used. The choice of the proper tolerance of the algorithm was based on the logic of conservation of each line's nature and the elimination of slight irregularities. Indicatively, in Figure 7 the mixed area's smoothed depth surface, the contours that stem from this surface and the smoothed contours after the application of PAEK with the corresponding tolerance, are depicted. According to the filtered depth surfaces in the sea grass area the depths vary from -1.4m to -5.5m, in the sandy area from -7.0m to -12.3m and in the mixed area from -2.9m to -6.8m.

6. Conclusions and discussion

Despite what was said in §4.2, about the multiplicity of bands that contributes to overcoming the problem of heterogeneous bottom types, the reality proved different. In this work, it is evident that the variety of the bottom cannot always be overcome by using more than two bands, even if we keep the assumption that the water is clear with the same properties throughout the study area. Especially when the bottom is covered with sea grass the problem becomes more intense since the sea grass absorbs the radiation. As it was shown in §4.3 the calibration of linear model in the whole of the study area was not statistically proper. Thus, it was decided the study area to be divided into three different sub-regions. However the separation into regions in order an acceptable calibration of the Lyzenga model to be produced, is something that is a major disadvantage in using these methods for the creation of a single bathymetric map for the whole study area. Nevertheless, the procedure was kept on in the three different areas in order the relevant experience to be obtained. A significant factor that introduced uncertainty into the results, was the original image's quality (§2). Moreover, the process of the bands' preparation, depended on parameters about which the researcher had to decide, like: the size and location of the image samples for the application of the Hedley's method, the value of the dark pixel (§3) for the crude atmospheric correction, or the values of the statistical indices according to which the result of the stepwise regression was accepted or not. Another factor that influenced the results was the image's resolution. Ikonos-2 is a high resolution image. For the purpose of the specific task, this can be either an advantage or a disadvantage. With the high resolution, we have a better matching of x,y coordinates of calibration points and corresponding pixels. This leads to a more appropriate calibration. Furthermore, the identification of small marine data, which can be a problem in navigation, is possible. On the other hand, the high resolution of the image returns more accurately the differences of the seabed. These differences however, apart from affecting the performance of the model, are quite intense and create a very dense raster surface with abrupt changes in depth from pixel to pixel. This necessarily, leads us to use smoothing filters for the raster surface. At this part of the process, the difficulty of choosing the appropriate spatial filter comes in, since the filter must return, as much as possible, the reality without deletions of useful information. Without a selection rule, the filter must be chosen with care and after many tests, while the researcher must be familiar with the phenomenon which is being smoothed.

In conclusion, the procedure for calculating depths, as seen from the literature (§1) is a fast and successful one, according to many researchers. The great advantage is that through the multispectral bathymetry very fast and relatively inexpensively depths at many points can be simultaneously calculated. At the same time, the calibration of the linear depth model or another model (e.g. Stumpf et al, 2003) needs few points of known depth, whose number is much less than the number which

should be measured for a classical bathymetric mapping. However, it is obvious that such a methodology is quite unstable, since many uncertainty factors are involved, acting with different weight in the individual conditions of each study area and influencing the calculation of accurate depths as well as their final digital cartographic exploitation.

References

Benny A.H. and Dawson G.J., 1983. *Satellite imagery as an aid to bathymetric charting in the Red Sea*, Cartographic Journal, 20:5-16

Bramante J., Raju D. K. and Min S.T., 2010. *Derivation of bathymetry from multispectral imagery in the highly turbid waters of Singapore's south islands. A comparative study*. http://dgl.us.neolane.net/res/img/ac5893d9670eb994050a72130f44f444.pdf

Conzales R.C. and Wintz P., 1987. *Digital Image Processing,* Adison Wesley, N.York

Doxani G., Papadopoulou M., Lafazani P., Pikridas C. and Tsakiri-Strati M., 2012. *Shallow-water bathymetry over variable bottom types using Multispectral worldview-2 image*, International Archives of the Photogrammetry, Remote Sensing and Spatial Information Sciences, Volume XXXIX-B8, 2012 XXII ISPRS Congress, 25 August – 01 September 2012, Melbourne, Australia

Doxani G., Papadopoulou M., Lafazani P., Tsakiri-Strati M. and Mavridou R.E., 2013. *Sun glint correction of very high spatial resolution images*, In: Arabelos D., Kaltsikis C., Spatalas S., Tziavos I.N. (eds), Thales, Honorary volume for professor Emeritus M.Kontadakis, Ziti, pp. 329-240

Edwards A.J., 2010. *Les. 7: Compensating for variable water depth to improve mapping of underwater habitats. Why it is necessary*. Bilko module 7, UNESCO. http://www.noc.soton.ac.uk/bilko/module7/m7_15.php

ESRI, *Desktop Help 10.0-Simplify Line (Cartography)*. http://help.arcgis.com/en/arcgisdesktop/10.0/help/index.html#//007000000010000000

Fotiou A. and Pikridas C., 2006. *GPS and Geodetic Applications*, Ziti, Thessaloniki, Greece

Green E., Mumby P., Edwards A. and Clark C., 2000. *Remote Sensing handbook for Tropical Coastal Management*. Coastal Management Sourcebooks series, UNESCO Pub., Chapt. 8

Hatzigaki S., Karkani Z., Matziri M., Papadopoulou M., Tsakiri-Strati M., Tziavos I.N., and Zidrou E., 2000. *Multispectral Bathymetry Supported by Sounding and GPS Data*. Tech. Chron. Sci.J.TCG, I, 2, pp. 99-110

Hedley J.D., Harborne A.R. and Mumby P.J., 2005. *Simple and robust removal of sun glint for mapping shallow-water benthos.* Int. J. Remote Sensing*,* 26(10): 2107-2112.

Kerr, J. M., 2010. *Worldview-02 offers new capabilities for the monitoring of threatened coral reefs.* In N.S.U.-N.C.R. Institute, editor. http://www.digitalglobe.com/downloads/8bc/Kerr_2010_Bathymetry_fr om_WV2.pdf.

Lafazani P., 2003. *Methods of Geographical Analysis*, Lecture Notes, School of Rural and

Surveying Engineering, AUTH, Thessaloniki, Greece

Li Z., 2007, *Multiscale spatial representation*, CRC, N.York

Lyons M., Phinn S. and Roelfsema C., 2011. *Integrating Quickbird multi-spectral satellite and field data: Mapping bathymetry, Sea grass Cover, Sea grass species and change in Moreton bay, Australia in 2004-2007*. Remote Sens., 3:42-64.

Lyzenga D., 1978. *Passive remote sensing techniques for mapping water depth and bottom features*. Applied Optics, 17(3), pp. 379-383.

Lyzenga D., 1981. *Remote sensing of bottom reflectance and water attenuation parameters in shallow water using aircraft and Landsat data*. Int. J. Remote Sensing, 2(1):71-82.

Lyzenga D., 1985. *Shallow-water bathymetry using combined lidar and passive multispectral scanner data*. Int. J. Remote Sensing, 6(1):115-125.

Lyzenga D., Malinas N. and Tanis F., 2006. *Multispectral bathymetry using a simple physically based algorithm*. IEEE Transactions on Geoscience and Remote Sensing, 44(8):2251-2259.

Mavridou R. E., 2013. *Creation of digital bathymetric maps using multispectral bathymetry*, MSc Thesis, School of Rural and Surveying engineering, AUTH

McCoy I., Johnston K., Kopp S., Borup B., Willison J.and Payne B., 2002, *Using ArcGIS Spatial Analyst,* ESRI

Mishra D., Narumalani S., Lawson M. and Rundquist D., 2007. *Bathymetric mapping using IKONOS multispectral data*. GIScience and Remote sensing, 41(4):301-321.

Papadopoulou M. and Tsakiri-Strati M., 1998. *Shallow sea water bathymetry using TM multispectral data*. Tech. Chron. Sci.J.TCG, I(1):87-98. (in greek, extended english summary)

Philpot, W.D., 1989. *Bathymetric mapping with passive multispectral imagery*. Applied Optics. 28:1569–1578.

Spitzer, D., and R. W. J. Dirks, 1987. *Bottom Influence on the Reflectance of the Sea*. International Journal of Remote Sensing, 8(3): 279–290.

Stumpf R., Holderied K. and Sinclair M., 2003. *Determination of water depth with high-resolution satellite imagery over variable bottom types*. Limnol. Oceanogr., 48 (1, part 2): 547-556.

Su H., Liu H. and Heyman W., 2008. *Automated derivation for bathymetric information for multispectral satellite imagery using a non-linear inversion model*. Marine Geodesy, 31, pp.281-298.

van Hengel W. and Spitzer D., 1991. *Multi-temporal water depth mapping by means of Landsat TM*. Int. J. Remote Sensing, 12(4): 703-712.